JB
Journals.ASM.org

Identification of Ata, a Multifunctional Trimeric Autotransporter of *Acinetobacter baumannii*

Leticia V. Bentancor, Ana Camacho-Peiro, Cagla Bozkurt-Guzel, Gerald B. Pier, and Tomás Maira-Litrán

Channing Laboratory, Department of Medicine, Brigham and Women's Hospital, Harvard Medical School, Boston, Massachusetts, USA

Acinetobacter baumannii **has recently emerged as a highly troublesome nosocomial pathogen, especially in patients in intensive care units and in those undergoing mechanical ventilation. We have identified a surface protein adhesin of *A. baumannii*, designated the *Acinetobacter* trimeric autotransporter (Ata), that contains all of the typical features of trimeric autotransporters (TA), including a long signal peptide followed by an N-terminal, surface-exposed passenger domain and a C-terminal domain encoding 4 β-strands. To demonstrate that Ata encoded a TA, we created a fusion protein in which we replaced the entire passenger domain of Ata with the epitope tag V5, which can be tracked with specific monoclonal antibodies, and demonstrated that the C-terminal 101 amino acids of Ata were capable of exporting the heterologous V5 tag to the surface of *A. baumannii* in a trimeric form. We found that Ata played a role in biofilm formation and bound to various extracellular matrix/basal membrane (ECM/BM) components, including collagen types I, III, IV, and V and laminin. Moreover, Ata mediated the adhesion of whole *A. baumannii* cells to immobilized collagen type IV and played a role in the survival of *A. baumannii* in a lethal model of systemic infection in immunocompetent mice. Taken together, these results reveal that Ata is a TA of *A. baumannii* involved in virulence, including biofilm formation, binding to ECM/BM proteins, mediating the adhesion of *A. baumannii* cells to collagen type IV, and contributing to the survival of *A. baumannii* in a mouse model of lethal infection.**

Acinetobacter baumannii is a Gram-negative opportunistic pathogen that has recently emerged as a significant cause of nosocomial infections worldwide (54). Multidrug-resistant (MDR) *A. baumannii* infections tend to occur in debilitated patients, especially those in intensive care units (ICUs) and/or in the context of serious underlying disease, in patients subjected to invasive procedures, such as mechanical ventilation, or those undergoing long hospitalizations or being treated with broad-spectrum antibiotics (25, 39). The most common clinical manifestations of *A. baumannii* infections in the ICUs are ventilator-associated pneumonia (VAP) and bacteremia, which are associated with morbidity and mortality rates as high as 52% (12, 64). Other hospital-acquired *A. baumannii* infections include urinary tract infections, wound infections, and meningitis (55). In addition, *A. baumannii* infections have been a recurrent problem during wars and natural disasters (53, 76), and recently MDR *A. baumannii* has become a major pathogen found in combat-associated wounds in military personnel deployed to Iraq or Afghanistan (18, 29). Problematically, 89% of *Acinetobacter* strains isolated from patients injured in Iraq and Afghanistan were resistant to at least two major classes of antibiotics (72). The lack of new antibiotics to treat MDR *A. baumannii* infections has led the Infectious Disease Society of America (IDSA) to describe *A. baumannii* as "an emblematic case of the mismatch between unmet medical needs and the current antimicrobial research and development pipeline" (48).

Although *A. baumannii* is a pathogen of considerable health care interest, surprisingly little is known about this organism's virulence determinants, bacterial regulatory networks, and host defense mechanisms. Recent DNA genome sequencing revealed that this organism harbors an extraordinary number of putative virulence-associated genes and elements homologous to the *Legionella*/*Coxiella* type IV secretion apparatus (66). Several virulence determinants involved in biofilm formation (24, 41), iron acquisition (79), lipopolysaccharide (LPS) synthesis (62), resistance to the bactericidal activity of human serum (33), adherence, host cell invasion (11, 42), and death (9, 10, 35) have been reported in previous studies. While these presumably encompass just a minor fraction of elements involved in *A. baumannii* virulence, new approaches are needed to expand our understanding of the basic features of this organism which will ultimately be essential to control the spread of *A. baumannii* infections and to develop effective means to prevent and/or treat this harmful pathogen.

To gain greater insight into *A. baumannii* virulence factors, we identified an ORF in *A. baumannii* ATCC 17978, A1S_1032, that codes for a protein belonging to the trimeric autotransporter (TA) family, which was termed the *Acinetobacter* trimeric autotransporter, or Ata. TAs encompass a large family of proteins produced by many Gram-negative bacteria that contain a C-terminal domain that is believed to form the trimeric β-barrel that allows for the transport of the N-terminal passenger domain to the bacterial cell surface. These proteins form lollipop-shaped surface projections on the bacterial surface and have been extensively studied as vaccine candidates against multiple pathogens (52). Two relevant examples of TAs as vaccine components include the *Neisseria meningitidis* NadA autotransporter (AT) which is undergoing phase III clinical evaluation against serogroup B meningococcal disease (65), and the conventional AT pertactin, produced by *Bordetella pertussis* strains (30), that is a component of four out of the five pertussis vaccines currently licensed for use in the United States (1).

In this report, we conducted an *in silico* structural analysis of the Ata protein and investigated its role in biofilm formation,

Received 9 April 2012 **Accepted** 14 May 2012
Published ahead of print 18 May 2012
Address correspondence to Tomás Maira-Litrán, tmaira@rics.bwh.harvard.edu.
Supplemental material for this article may be found at http://jb.asm.org/.

doi:10.1128/JB.06769-11

TABLE 1 Bacterial strains and plasmids used in this work

Strains and plasmids	Description	Source or reference
A. baumannii strains		
ATCC 17978	Reference sequenced strain, susceptible to antibiotics	ATCC
ATCC 17978 Δ*ata*	ATCC 17978 derivative with an in-frame deletion of *ata*	This work
ATCC 17978 Δ*ata*-c	ATCC 17978 Δ*ata* complemented with pBAD-Ata	This work
ATCC 17978 Δ*ata*-pLVB-Ata	ATCC 17978 Δ*ata* complemented with pLVB-Ata	This work
ATCC 17978 Δ*ata*-pBAD18kan-Ori	ATCC 17978 Δ*ata* complemented with pBAD18kan-Ori	This work
E. coli strains		
DH5α λ*pir*	λ*pir* lysogen of DH5α	Laboratory strain
LMG194	F$^-$ Δ*lacX74 galE thi rpsL* Δ*phoA* (PvuII) Δ*ara714 leu*::Tn*10*	Invitrogen
Top10	Used as host for gene cloning	Invitrogen
Plasmids		
pSSK10	Derived from pDS132 (*R6K ori mobRP4 cat sacB*), Km^r	66
pCR-XL-TOPO	PCR cloning plasmid, Km^r	Invitrogen
pΔ*ata*	pSSK10 carrying an ~3.4-kb fragment of the 5′ and 3′ flanking regions of *ata*	This work
pBAD18kan-Ori	*E. coli-Acinetobacter* shuttle vector	8
pBAD-Ata	*A. baumannii* ATCC 17978 promoterless *ata* gene (5,682 bp) cloned in pBAD18Kan-Ori	This work
pBAD-TOPO-TA	Protein expression vector carrying C-terminal V5-6×His tag; Ap^r	This work
pBAD-SP	Promoter and signal peptide of *ata* cloned in pBAD-TOPO-TA	This work
pBAD-TD	Translocator domain of *ata* cloned in pBAD18Kan-Ori	This work
pAta-V5-6×His	SP-V5-6×His fragment cloned in pBAD-TD	This work
pAta	pBAD-TOPO derivative carrying 5,274-bp coding sequence coding for the passenger domain of *ata*	This work
pTOPO-XL-Ata	*A. baumannii* ATCC 17978 *ata* gene with its own promoter (5,789 bp) cloned in pCR-XL-TOPO	This work
pLVB-Ata	*ata* from pTOPO-XL-Ata cloned in pBAD18kan-Ori	This work

binding to extracellular matrix/basal membrane (ECM/BM) proteins, and adhesion of whole *A. baumannii* cells to collagen type IV, as well as in virulence in a mouse model of lethal infection in immunocompetent mice.

MATERIALS AND METHODS

Bacterial strains and growth conditions. The bacterial strains and plasmids used in this study are listed in Table 1. All strains were routinely grown in lysogeny broth (LB) with the exception of *Escherichia coli* LMG194, which was grown in M9 minimal medium supplemented with 0.25% Casamino Acids. Carbenicillin and kanamycin were added to the growth medium at 50 μg/ml each.

Bioinformatics. The signal peptide and secondary structure features of Ata were predicted using the SignalP 3.0 program, available at http://www.cbs.dtu.dk/services/SignalP/ (2), and the PSIPRED software (38), respectively.

A model of the three-dimensional (3D) structure of the C-terminal 101 Ata residues was built by the combined use of homology modeling and molecular mechanics. A homology model of the Ata membrane anchor was built in CPH-models (51) using the crystal structure of the membrane anchor of *Haemophilus influenzae* Hia protein as a template. DeepView software (27) was used for construction of the homology model and for manipulation of torsion angles.

Construction of strains. We constructed a vector to generate an in-frame deletion of *ata* in *A. baumannii* ATCC 17978 in the following manner. An approximately 3.4-kb fragment of the 5′ and 3′ regions of *ata* were amplified by PCR using the primer pairs NdeI-Ata-3.4-F/MluI-Ata-R and MluI-Ata-F/XhoI-Ata-3.4-R, respectively (Table 2). The fragments were then digested with NdeI/MluI and MluI/XhoI and ligated between the NdeI and XhoI sites of pSSK10 (68). The resulting plasmid, pΔ*ata*, contained approximately 3.4 kb of DNA flanking regions on both sides of *ata*. ATCC 17978 Δ*ata*, harboring an in-frame deletion of *ata*, was made by first transforming pΔ*ata* into *A. baumannii* strain ATCC 17978 by electroporation. Clones in which the plasmid was integrated into the chromosome were selected on LB agar plates supplemented with kanamycin. *A. baumannii* ATCC 17978 merodiploids were grown for 2 days in LB without antibiotic selection, plated on LB agar supplemented with 10% sucrose, and grown at 25°C for 48 h to select for cells that had lost the plasmid after homologous recombination. Kanamycin-sensitive, sucrose-resistant colonies were screened by PCR using primers Ata-F-out/Ata-R-out to confirm deletion of *ata*. In-frame deletion of the *ata* gene was confirmed by sequencing using primers Ata-F-out/Ata-R-out. The resulting strain contains the first 13 and last 3 amino acids (aa) of the *ata* product in frame.

Complementation plasmid pBAD-Ata was constructed as follows. The *ata* gene was amplified by PCR with the KAPA HiFi DNA polymerase (Kapa Biosystems) from the chromosomal DNA of *A. baumannii* ATCC 17978 using primers XbaI-Ata-C-F and SphI-Ata-C-R. The resulting 5,682-bp DNA fragment was then digested with XbaI/SphI ligated between the XbaI and SphI sites of pBAD18kan-Ori to produce the plasmid pBAD-Ata, which was then transformed into *A. baumannii* ATCC 17978 Δ*ata* by electroporation, generating strain ATCC 17978 Δ*ata*-c.

To construct the complementation plasmid pLVB-Ata containing *ata* with its own promoter, the *ata* gene was amplified by PCR with the KAPA HiFi DNA polymerase (Kapa Biosystems) from the chromosomal DNA of *A. baumannii* ATCC 17978 using primers Ata-C2-F and Ata-C2-R. Following amplification, the resulting 5,789-bp PCR product was mixed with 2.5 U of *Taq* DNA polymerase (Invitrogen) and 2 mM dATP in 1× *Taq* buffer and incubated at 72°C for 10 min to allow addition of 3′ A-overhangs before *ata* was subcloned into the pCR-XL-TOPO vector to generate pTOPO-XL-Ata. Ligation of DNA into pCR-XL-TOPO and subsequent transformation into *E. coli* TOP10 cells were performed according to the manufacturer's protocol. The *ata* gene was then isolated from pTOPO-XL-Ata after digestion with EcoRI and cloned into the EcoRI-digested shuttle vector pBAD18kan-Ori to generate the complementation vector pLVB-Ata. Finally, the pLVB-Ata plasmid was introduced in *E. coli* TOP10 cells by electroporation. Primers pBAD-R and Ata-C2-R were then used to deliberately select a clone where the orientation of *ata* in

TABLE 2 Oligonucleotide primers used in this study

Primer name	Sequence (5′ to 3′)[a]	Purpose
NdeI-Ata-3.4-F	GGGCCCCATATGGGGCATAAAAAACGCAGTCCAAAAAACGGTG	Clone 5′ upstream region of *ata*
MluI-Ata-R	GGGCCCACGCGTAATCGAAGCATTCCAAATGACCTTGTAAAC	Clone 5′ upstream region of *ata*
MluI-Ata-F	GGGCCCACGCGTATTAATTAAGAAACTGGTTGGGAGGGCAAT	Clone 3′ downstream region of *ata*
XhoI-Ata-3.4-R	GGGCCCCTCGAGAGAGCTTCGGCTGATTGAACAAACTTTTAGG	Clone 3′ downstream region of *ata*
Ata-F-out	ATTTATTCAATTAGGATGCCGCCTCTTTTTTTGG	Confirm in-frame deletion of *ata*
Ata-R-out	CTAAGACTAAGCTTTGGATTGTTTTGTTCATCTC	Confirm in-frame deletion of *ata*
XbaI-Ata-C-F	GGGCCCTCTAGATTGGTCGTTGAGTTCG	Complementation of *ata*
SphI-Ata-C-R	GGGCCCGCATGCTTAATTAATCACACCACTAATACCA	Complementation of *ata*
Ata-SP-F	TATTTGTCTGAGAAGTTTTATGAATAAAGTTTACAAGG	Amplification of promoter and signal peptide of *ata*
Ata-SP-R	AGCAAAAGCATTTGGAGCAAAACAAATTACACCC	Amplification of promoter and signal peptide of *ata*
KpnI-TD-F	GGGCCCGGTACCAACAAAATTACCAATCTGGGTGATCAGTTACAA	Amplification of *ata* translocator domain
SphI-TD-R	GGGCCCGCATGCTTAATTAATCACACCACTAATACCAACGCGGAC	Amplification of *ata* translocator domain
SacI-SP-V5-6×His-F	GGGCCCGAGCTCTATTTGTCTGAGAAGTTTTATGAATAAAGTTTACAAG	Amplification of *ata* promoter-signal peptide-V5-6×His
KpnI-SP-V5-6×His-R	GGGCCCGGTACCATGGTGATGGTGATGATGACCGGTAC	Amplification of *ata* promoter-signal peptide-V5-6×His
NdeI-Ata-PD-F	GGGCCCCATATGGGGACAAATACCGAAGGGGGAATAG	Cloning passenger domain of *ata*
XhoI-Ata-PD-R	GGGCCCCTCGAGTTCTAAGGCCATGGCAGCG	Cloning passenger domain of *ata*
Ata-C2-F	ATTTATTCAATTAGGATGCCGCCTCTTTTTTTGG	Complementation of *ata* with its native promoter
Ata-C2-R	CTAAGACTAAGCTTTGGATTGTTTTGTTCATCTC	Complementation of *ata* with its native promoter
pBAD-R	CCGCCAGGCAAATTCTGTTTTATCAG	Confirm orientation of *ata* in pLVB-Ata vector

[a] Restriction sites are underlined.

pBAD18kan-Ori was in the opposite direction of the pBAD promoter and therefore where the expression of *ata* was controlled by its own native promoter rather than by the pBAD promoter. pBAD18kan-Ori was chosen to construct the complementation plasmid pLVB-Ata mainly for its ability to replicate in *E. coli-A. baumannii* and its stability *in vivo* rather than for its arabinose-inducible pBAD promoter. The pLVB-Ata plasmid was finally electroporated into *A. baumannii* Δ*ata* cells to generate the complemented strain *A. baumannii* Δ*ata*-pLVB-Ata.

The control strain *A. baumannii* Δ*ata*-pBAD18kan-Ori was prepared by electroporating the empty vector pBAD18kan-Ori into the mutant strain *A. baumannii* ATCC 17978 Δ*ata*.

Replacement of the Ata passenger domain with the V5-6×His epitope tags. The V5-6×His peptide was fused to the C-terminal region of Ata according to the following steps. First, a fragment containing the promoter and signal sequence of *ata* was amplified by PCR, with primers Ata-SP-F and Ata-SP-R, and ligated upstream of the V5-6×His sequence contained in the plasmid pBAD-TOPO-TA to generate the plasmid pBAD-SP. A second PCR amplicon containing the predicted translocator domain of *ata* was amplified with primers SphI-TD-R/KpnI-TD-F digested with SphI and KpnI and cloned into SphI/KpnI digested pBAD18Kan-Ori to generate pBAD-TD. The entire *ata* promoter-SP-V5-6×His fragment then was amplified from pBAD-SP with primers SacI-SP-V5-6×His-F and KpnI-SP-V5-6×His-R, cloned in the SacI/KpnI-digested pPBAD-TD to generate fusion plasmid pAta-V5-6×His, and introduced into *E. coli* LMG194 by electroporation. All constructs were examined by nucleotide sequencing to ensure that the inserts were in frame and that all PCR products were free of mutations.

Immunoblotting. *E. coli* LMG194 pAta-V5-6×His cells were grown in M9 plus 0.25% Casamino Acids and induced with either 0.2% arabinose or 0.2% glucose for 4 h. Outer membrane fractions of whole-cell bacterial sonicates were prepared on the basis of Sarkosyl insolubility as described previously (19). The samples were resuspended in SDS-PAGE loading buffer, boiled for 5 min, and separated on a 10% Bis-Tris gel (Invitrogen) using morpholineethanesulfonic acid (MES) running buffer. Proteins were transferred to Invitrolon polyvinylidene difluoride (PVDF) membranes (Invitrogen) and blocked with phosphate-buffered saline (PBS)–5% nonfat dry milk for 1 h at room temperature. Blocked membranes were incubated for 1 h with mouse IgG1 anti-V5 monoclonal antibody (MAb) (Santa Cruz Biotechnology) diluted 1:1,000 in PBS plus 0.05% Tween 20 (PBST)–2% nonfat dry milk. V5 epitopes were detected with goat anti-mouse IgG (Southern Biotech) (1:1,000 dilution in PBST–2% nonfat dry milk) by enhanced chemiluminescence (Western blotting reagent; Santa Cruz Biotechnology). Some arabinose-induced pAta-V5-6×His outer membrane protein (OMP) samples were also subjected to depolymerization by overnight treatment with 70% formic acid at room temperature as described elsewhere (69) and then analyzed by Western blotting as described before.

To investigate the levels of Ata expression among clinical isolates by Western blotting, cultures of eight *A. baumannii* clinical strains (ATCC 17978, S19, I30, N10, I42, I25, I31, and I28) as well as the *ata*-negative strain ATCC 17978 Δ*ata* were grown in LB to an optical density at 650 nm (OD_{650}) of 0.025, and OMPs were extracted and processed as described above for the strain *E. coli* LMG194 pAta-V5-6×His. Purified OMPs (2.5 μg) were resolved on a 4 to 12% Bis-Tris gel using morpholinepropanesulfonic acid (MOPS) running buffer, transferred to PVDF membranes, and analyzed by Western blotting as before but using rabbit sera raised to Ata (1:1,000 dilution) as the primary antibody and a secondary goat anti-rabbit IgG (Southern Biotech) diluted 1:1,000.

Purification of recombinant Ata. The passenger domain of Ata was PCR amplified from the genomic DNA of *A. baumannii* strain ATCC 17978 with primers NdeI-Ata-PD-F/XhoI-Ata-PD-R, digested with NdeI and XhoI, and cloned into NdeI/XhoI-digested pBAD-TOPO-TA (Invitrogen) to generate pAta. Recombinant protein expression from pAta was induced in *E. coli* TOP10 cultured to an OD_{650} of 0.4 in LB containing carbenicillin by addition of 2% L-arabinose and further incubation for 4 h. Soluble His-tagged Ata was purified by affinity chromatography on a nickel column according to the protocols of the manufacturer (Novagen). The purity was checked by SDS-PAGE stained with Coomassie blue, and protein content was quantified with the Bradford assay (3).

Biofilm formation. *A. baumannii* overnight cultures were diluted 1:100 in 2 ml of either fresh LB (ATCC 17978 and Δ*ata* strains) or LB plus 2% arabinose or 0.2% glucose (Δ*ata*-c strain), and biofilms were allowed to form in polystyrene plastic tubes under static conditions for 24 h. At this point, the cultures were monitored for planktonic growth by measuring the OD_{650}. Once the medium and planktonic cells were removed, biofilms were gently washed with PBS to remove loosely attached cells, dried, and stained with a 0.2% crystal violet solution. After biofilms were rinsed with deionized water, the biomass was quantified by adding 2 ml of

100% ethanol and vortexing until the stained biomass was completely removed from the tube surface, and the OD_{595} was determined (8). Biofilm formation was expressed as a normalized value: OD_{595} divided by the planktonic cell density (OD_{650}) of each tube.

Flow-cytometric analysis of bacterial production of Ata. Flow cytometry was used to examine the production of Ata by *A. baumannii* ATCC 17978 at various phases of growth, from early exponential to stationary phase, to optimize the induction/repression conditions from the complementation vector pBAD-Ata as well as to compare Ata production in wild-type *A. baumannii* ATCC 17978 to that in Δ*ata*, Δ*ata*-pLVB-Ata, and Δ*ata*-pBAD18kan-Ori strains and among *A. baumannii* clinical isolates.

To investigate the production of Ata during all phases of growth, wild-type *A. baumannii* ATCC 17978 was grown to an OD_{650} of 0.025, 0.1, 0.4, 0.8, and 1.2, whereas for the optimizing of Ata production from pBAD-Ata, Δ*ata*-c cells were grown to an OD_{650} of 0.4 and induced for 2 h with arabinose or glucose at concentrations ranging from 0.2 to 2%. After cells were washed with PBS, the OD_{650} of all samples was adjusted to 0.4, and then they were incubated for 1 h at room temperature with rabbit sera raised to recombinant Ata (1:1,000 dilution in PBS) that had been previously absorbed with the *A. baumannii* ATCC 17978 Δ*ata* strain to remove any reactivity to antigens other than Ata. Following three washes with PBST, cells were incubated for 30 min with Alexa 488-conjugated goat antibody to rabbit IgG (Invitrogen) diluted 1:250 in PBS. Bacterial cells were washed three times with PBST and then analyzed by a FACSCalibur flow cytometer (Becton, Dickinson). We found that the induction of *A. baumannii* ATCC 17978 Δ*ata*-c with 2% arabinose for 2 h resulted in high levels of surface Ata, comparable to those seen in the wild-type strain grown to an OD_{650} of 0.025, whereas growth with 0.2% glucose was optimal for maximum repression of *ata* expression from the recombinant plasmid. Therefore, these concentrations of arabinose and glucose were used as our standard induction/repression conditions for the complementation vector pBAD-Ata throughout this study (data not shown).

Finally, for testing the levels of Ata in *A. baumannii* ATCC 17978, Δ*ata*, Δ*ata*-pLVB-Ata, and Δ*ata*-pBAD18kan-Ori and among *A. baumannii* clinical isolates, bacteria were grown to an OD_{650} of 0.025 and washed with PBS. After the OD_{650} was adjusted to 0.4, samples were processed as described above for analysis by fluorescence-activated cell sorting (FACS).

Quantitative real-time PCR (qRT-PCR). *A. baumannii* ATCC 17978 cells grown to early log (OD_{650} of 0.1) and mid-log (OD_{650} of 0.4) phase were harvested with RNA Protect (Qiagen), and total RNA was isolated using the RNeasy kit (Qiagen) according to the manufacturer's recommendations. Genomic DNA was removed by incubating the samples twice with Turbo DNase at 37°C for 30 min according to the manufacturer's instructions (Ambion). One microgram of RNA was used to synthesize cDNA using the SuperScript III first-strand synthesis system (Invitrogen), and quantitative analysis of cDNAs was performed with a Light Cycler 480 system instrument using SYBR green I master mix (Applied Biosystems) to detect PCR products. Primers for PCR were designed to amplify a product of approximately 200 bp with the primer3 software. Reactions were set up according to the manufacturer's instructions, and three replicates for each sample were included. The amplification conditions were 95°C for 5 min (ramp rate of 4.5°C/s), followed by 45 cycles of 95°C for 10 s (ramp rate of 4.5°C/s), 55°C for 20 s (ramp rate of 2.5°C/s), and 72°C for 30 s (ramp rate of 4.5°C/s). The specificity of the reaction was confirmed by obtaining a melting curve from 95 to 55°C. The threshold cycle (C_T) value was defined as the cycle in which the fluorescence value was above the background level. Relative gene expression was quantified using the $2^{-\Delta\Delta CT}$ method (44) with the 16S rRNA gene as a control for normalization.

CLSM. Confocal laser-scanning microscopy (CLSM) was used to evaluate the surface localization of the Ata-V5-His fusion protein on *E. coli* pAta-V5-6×His as well as the production of Ata in *A. baumannii* ATCC 17978, Δ*ata*, and Δ*ata*-c strains. *E. coli* pAta-V5-6×His cells were grown to an OD_{650} of 0.4 and induced for 4 h with either 0.2% arabinose or 0.2% glucose. For *A. baumannii* strains, cells were grown to an OD_{650} of 0.025 (ATCC 17978 and Δ*ata*) or 0.4 and then induced for 2 h with either 2% arabinose or 0.2% glucose (ATCC 17978 Δ*ata*-c). Bacteria were washed with PBS, and the OD_{650} of all samples was adjusted to 0.4. Cells were then incubated for 15 min in blocking buffer (PBS–5% bovine serum albumin [BSA]) and then with a 1:100 dilution of anti-V5 MAb or 1:50 dilution of polyclonal rabbit antiserum raised against Ata. Finally, cells were incubated with a 1:200 dilution of a secondary antibody coupled to Alexa 488 along with 1 μg/ml of 4′,6-diamidino-2-phenylindole (DAPI) in PBS. Following three washes with PBS, bacteria were analyzed by CLSM as described elsewhere (8).

Binding of Ata to ECM/BM proteins. Microtiter plates were coated overnight at 4°C with 5 μg of fibronectin, laminin, heparan, collagen types I, II, III, IV, and V (all from Sigma), vitronectin (R&D Systems), or BSA (Sigma) per well in 100 mM phosphate buffer, pH 7. Wells were washed three times with PBST and then treated with blocking solution (PBST–2% nonfat dry milk) for 2 h at 37°C. After three washes with PBST, 50 μl of purified recombinant Ata (0.02 to 2.5 μg/ml) diluted in PBS plus 0.1% blocking solution was added to the plate wells and incubated at 37°C for 2 h. After three washes with PBST, wells were incubated at 37°C for 1 h with rabbit antiserum diluted 1:1,000 in 0.1% blocking solution. Following three washes in PBST, wells were incubated with a secondary anti-rabbit antibody (alkaline phosphatase conjugated and diluted 1:1,000) in 0.1% blocking solution at 37°C for 1 h. Once wells were washed three times with PBST, the binding of Ata was detected with p-nitrophenyl phosphate (pNPP) substrate by measuring the absorbance at 405 nm.

Binding of *A. baumannii* to collagen type IV. Microtiter tissue culture plates were coated with collagen type IV, blocked, and washed as described before. *A. baumannii* ATCC 17978, Δ*ata*, and Δ*ata*-c strains induced with arabinose or glucose were grown as described above and resuspended in phosphate-buffered saline (PBS) to an OD_{650} of 0.4. One hundred μl containing 5×10^6 CFU was added to each well and incubated for 1 h at 37°C. Wells were rinsed four times with PBS and treated with trypsin-EDTA to release the bound bacteria. The number of adherent *A. baumannii* cells was determined by serial dilution and plating.

Rabbit antibodies to Ata and enzyme-linked immunoabsorbent assay (ELISA). Antibodies to recombinant Ata were raised in rabbits after immunization with 10-μg doses of recombinant Ata by following protocols described elsewhere (47).

***A. baumannii* virulence studies.** The role of Ata in *A. baumannii* virulence was investigated in a recently developed lethal model of systemic infection (4). In this model, wild-type *A. baumannii* ATCC 17978, Δ*ata*, Δ*ata*-pLVB-Ata, or Δ*ata*-pBAD18kan-Ori were grown to an OD_{650} of 0.025, washed once with PBS, and used to infect groups of immunocompetent mice (C57BL/6; female; $n = 8$; 3 to 5 weeks of age) intraperitoneally (i.p.) with a dose of approximately 10^7 CFU per animal. Mortality was scored for a 5-day period.

Statistical analysis. All statistical analyses were performed using Prism 4.0 (GraphPad Software). Results from comparisons of biofilm formation and binding to collagen IV for *A. baumannii* strains were analyzed by one-way analysis of variance (ANOVA) with Tukey's correction. Survival data for the different mouse groups were analyzed by using Kaplan-Meier survival curves and the log-rank test. A P value of <0.05 was considered significant

Accession numbers. The complete genome sequence and annotation of *A. baumannii* ATCC 17978 has been deposited in the GenBank/EMBL/DDBJ database under accession no. CP000521. The nucleotide and predicted amino acid sequence accession numbers of the *ata* gene and protein are CP000521 and ABO11464, respectively.

RESULTS

***In silico* predicted structure of Ata.** The 5,622-bp *ata* gene, ORF A1S_1032, from *A. baumannii* ATCC 17978 is predicted to encode a protein that shares many structural features with the other AT

proteins, including YadA from *Yersinia enterocolitica*, NhhA from *N. meningitidis*, or Uspa1 from *Moraxella catarrhalis* TA proteins, among others.

Signal peptide and secondary structure prediction analysis of Ata revealed that this protein contains a long putative signal sequence with a signal peptidase cleavage site predicted to be between amino acids 53 and 54 that was followed by a large N-terminal passenger domain (amino acids 54 to 1772) containing four pentameric collagen binding consensus sequences (SVAIG) and one Arg-Gly-Asp (RGD) motif. The 101-amino-acid C-terminal sequence of Ata is predicted to contain a translocator domain that can be separated into an initial 39-amino-acid α-helix and a 9-amino-acid hairpin loop that connects the α-helix to the β-barrel domain. The β-barrel domain is predicted to contain four transmembrane antiparallel β-sheets (β1 to β4) of 9, 10, 10, and 11 amino acids connected by short turns (see Fig. S1A in the supplemental material). By analogy to other members of the TA family, the trimerization of this region in the outer membrane may form 12-stranded pore-forming β-barrels containing four strands from each of three subunits to mediate the exposure of the N-terminal part of the protein at the cell surface.

Based on results from secondary structure predictions and the strong amino acid sequence similarity of Ata to other TAs, we generated a computer model of the putative 3D structure of the last 101 amino acids of Ata with the Chimera computer modeling tool (16, 56) using the crystal structure of Hia (Protein Data Bank identification no. 2GR7) as a template. Figure S1B in the supplemental material represents an overview of the modeled structures of monomeric and trimeric Ata. The three individual α-domains for each Ata monomer are predicted to be exposed at the surface of the structure, looping out of the 12-stranded β-barrel pore formed with four antiparallel β-sheets from each of the monomers of Ata.

The C-terminal 101-amino-acid region of Ata contains functional translocator activity. Results from the *in silico* analysis of Ata suggested that the C-terminal region of Ata contains the translocator activity of the protein. To test this hypothesis, we investigated if the C-terminal 101 amino acid residues of Ata, predicted to contain the translocator function, were capable of presenting a heterologous passenger domain on the bacterial surface using a fusion protein, Ata-V5-His. After induction of *E. coli* pAta-V5-6×His cells with either 2% arabinose or 0.2% glucose, extraction of the OMPs, and analysis by Western blotting with anti-V5 MAbs, we found that OMP extracts from arabinose-induced *E. coli* cells had an anti-V5 reactive band that ran between 38 and 49 kDa (Fig. 1A, lane 2). No bands were visible when *E. coli* was grown under the repressing conditions containing glucose (Fig. 1A, lane 1). As the predicted size of the mature monomeric Ata-V5-His fusion protein is approximately 13.8 kDa, it appears that the V5 band observed was a trimer of the Ata-V5-His fusion protein. Previous accounts indicated that C termini of other AT proteins, such as Hia and YadA, formed heat-resistant, sodium dodecyl sulfate-resistant trimers in the outer membrane, and that Hia requires formic acid denaturation for dissociation (61, 70). After treatment of our samples with 70% formic acid overnight at room temperature, we found that OMP samples from arabinose-grown *E. coli* pAta-V5-6× had an altered migration of the V5 reactive band that ran at approximately 14 kDa, a size consistent with a monomer of the Ata-V5-His protein (Fig. 1A, lane 3). Similar results were obtained when Western blottings were probed with anti-His MAbs (data not shown).

We next used CLSM to confirm the surface location of the Ata-V5-His chimeric protein in arabinose- or glucose-induced *E. coli* pAta-V5-6×His cells. As shown in Fig. 1B, high levels of labeling were observed in arabinose-induced *E. coli* pAta-V5-6×His (Fig. 1B, panel a) but not when the *E. coli* cells were grown under repressing effects of glucose (Fig. 1B, panel b). Control DAPI-stained *E. coli* pAta-V5-6×His cells induced with arabinose or glucose are shown in panels c and d, respectively.

The surface localization of Ata in *A. baumannii* cells was further confirmed by CLSM studies using wild-type *A. baumannii* ATCC 17978, Δ*ata*, and Δ*ata*-c strains grown in the presence of arabinose or glucose. Results presented in Fig. 1C demonstrated high levels of surface Ata production in both wild-type *A. baumannii* ATCC 17978 (Fig. 1C, panel a) and arabinose-induced Δ*ata*-c (Fig. 1C, panel d) but not in the Δ*ata* strain (Fig. 1C, panel b) or the glucose-induced Δ*ata*-c strain (Fig. 1C, panel c).

All CLSM studies with *E. coli* pAta-V5-6×His and *A. baumannii* ATCC 17978, Δ*ata*, and Δ*ata*-c were carried out with intact, nonpermeabilized cells.

In summary, the Western blot analysis of OMP extracts from the Ata-V5-His fusion protein demonstrated that ORF A1S_1032 encodes a TA protein, and CLSM confirmed its surface localization.

Production of Ata is growth phase dependent. We investigated the production of Ata in *A. baumannii* ATCC 17978 at various growth phases in LB (OD_{650} of 0.025, 0.1, 0.4, 0.8, or 1.2) by measuring surface Ata production by flow cytometry. Results presented in Fig. 2 showed growth phase-dependent Ata production, with the highest levels found at very early exponential phase (mean fluorescence intensity [MFI], 574 at an OD_{650} of 0.025), followed by a continuous decline throughout the logarithmic and stationary phases. In contrast, the MFI levels of *ata*-negative strain ATCC 17978 Δ*ata* grown to an OD_{650} of 0.025, which was included as a control in these experiments, was only 7.6. Since *A. baumannii* ATCC 17978 and Δ*ata* differ only in the production of Ata, the differences in MFI levels observed (574 for *A. baumannii* ATCC 17978 and 7.6 for the *ata* mutant) validate the specificity of the primary antibodies used in these studies to the Ata protein.

In addition to FACS analysis, we investigated *ata* expression by quantitative real-time PCR (qRT-PCR) studies on *A. baumannii* ATCC 17978 cells grown to early log (OD_{650} of 0.1) and mid-log (OD_{650} of 0.4) phases in LB. Our results showed that the level of Ata mRNA was approximately 3-fold higher at an OD_{650} of 0.1 that at an OD_{650} of 0.4 (means ± standard deviations, 2.98 ± 0.1; $n = 3$ independent experiments). This pattern of *ata* transcription is consistent with our previous FACS results showing higher levels of Ata production in the early logarithmic phase and a continuous decline throughout the logarithmic and stationary phases.

Ata is critical for biofilm development of *A. baumannii*. The ability of bacteria to form biofilms is a trait closely associated with bacterial persistence and virulence (15, 21). We therefore investigated the role of *ata* in biofilm formation by *A. baumannii*. Results presented in Fig. 3 show that *A. baumannii* ATCC 17978 formed biofilms of adherent cells, while biofilm production was significantly lower in the ATCC 17978 Δ*ata* cultures ($P < 0.05$ by one-way ANOVA). Complementation of the biofilm-negative ATCC 17978 Δ*ata* strain with the *ata* gene in *trans* restored the biofilm-positive phenotype of the *A. baumannii* ATCC 17978 strain only

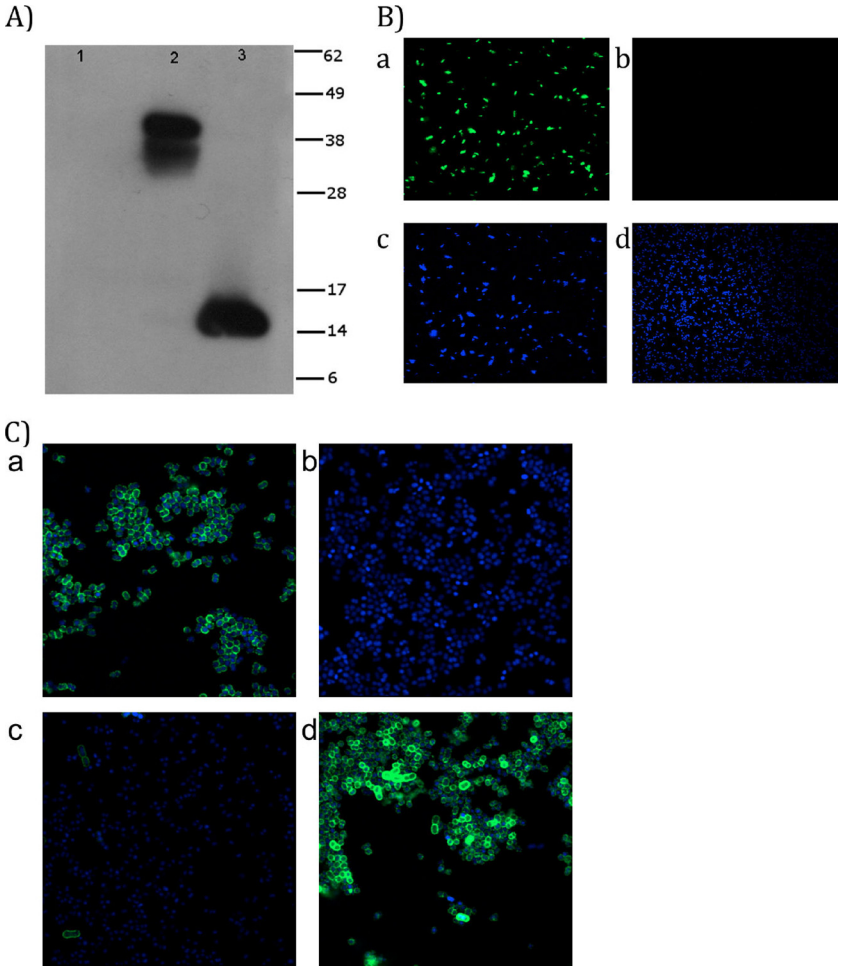

FIG 1 (A) Immunoblot of Ata-V5-His fusion protein expressed in *E. coli.* Outer membrane proteins (OMPs) of *E. coli* LMG194 harboring pAta-V5-6×His were prepared after induction with either 0.2% glucose (lane 1) or 0.2% arabinose (lane 2) and then tested by Western blotting with a monoclonal antibody (MAb) directed against the V5 peptide. Samples from arabinose-induced OMPs were treated with 70% formic acid and detected as before (lane 3). The predicted monomeric mass of Ata-V5-His fusion proteins is 13.8 kDa. Migration distances of molecular mass markers (in kDa) are indicated on the right. (B) Detection of Ata-V5-His fusion protein in *E. coli* pAta-V5-6×His by CLSM. *E. coli* pAta-V5-6×His cultures were grown in M9 plus 0.25% Casamino Acids and induced with 0.2% arabinose or 0.2% glucose. The V5 epitope was labeled with a mouse anti-V5 MAb and a secondary goat anti-mouse Alexa 488 fluorescent antibody (green channel), and cell nucleic acids were stained with DAPI (blue channel). (a) *E. coli* pAta-V5-6×His induced with arabinose (green channel) or (b) glucose (green channel). Also shown are DAPI-stained nuclei of *E. coli* cells (blue channel) after induction with arabinose (c) or glucose (d). (C) CLSM detection of Ata in *A. baumannii* ATCC 17978, Δ*ata*, and Δ*ata*-c strains. *A. baumannii* ATCC 17978, Δ*ata*, and Δ*ata*-c induced with arabinose or glucose were labeled with rabbit anti-Ata antisera and a secondary goat anti-rabbit Alexa 488 fluorescent antibody. Nucleic acids were stained with DAPI. Merged images of Alexa 488- and DAPI-stained *A. baumannii* ATCC 17978 (a) and Δ*ata* (b), Δ*ata*-c induced with glucose (c), and Δ*ata*-c induced with arabinose (d) are shown.

when cells were grown under arabinose-inducing conditions (for Δ*ata* versus Δ*ata*-c arabinose, $P < 0.001$ by one-way ANOVA) but not when they were incubated in the presence of the repressing effects of glucose (for Δ*ata* versus Δ*ata*-c glucose, not significant according to one-way ANOVA).

Ata binds multiple extracellular/basal matrix proteins and mediates the binding of *A. baumannii* to collagen type IV. As one of the main roles of TAs is to act as adhesins, facilitating the binding of bacteria to host tissues (43), we evaluated the ability of purified recombinant Ata to bind various ECM/BM proteins, including purified collagen types I, II, III, IV, and V, laminin, heparan, fibronectin, and vitronectin. As presented in Fig. 4A, there was a clear dose-dependent binding of recombinant Ata to collagen types I, III, IV, and V and laminin. There was no binding of Ata to collagen type II, fibronectin, vitronectin, or heparan, which was comparable to binding to the negative control, BSA.

We then investigated if, in addition to binding multiple ECM/BMs, Ata could promote the adhesion of whole *A. baumannii* cells to ECM/BMs. For this, we compared the binding of the wild-type *A. baumannii* ATCC 17978, Δ*ata*, and Δ*ata*-c strains grown in arabinose or glucose to immobilized collagen type IV, which was used as a prototype ECM/BM protein. Results presented in Fig. 4B demonstrate that the deletion of *ata* results in a significant decrease in the binding of *A. baumannii* ATCC 17978 cells to collagen IV-coated plates (for *A. baumannii* ATCC 17978 versus Δ*ata*, $P < 0.001$ by one-way ANOVA), and that this binding was restored when the Δ*ata*-c strain was grown under arabinose-inducing conditions (for Δ*ata* versus Δ*ata*-c-arabinose, $P < 0.01$ by one-way ANOVA) but not in the presence of repressive effects of glucose (for Δ*ata* versus Δ*ata*-c-glucose, not significant according to one-way ANOVA).

In conclusion, our results demonstrate that Ata not only binds

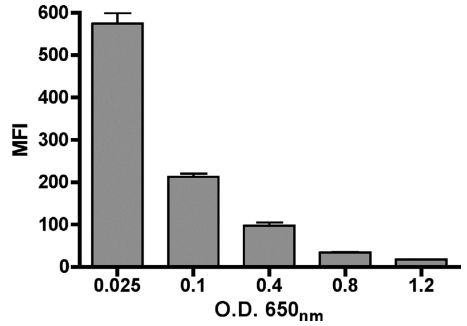

FIG 2 Quantification of Ata expression in *A. baumannii* ATCC 17978 by flow cytometry during various growth phases. *A. baumannii* was grown in LB to early exponential (OD_{650} of 0.025 or 0.1), mid-exponential (OD_{650} of 0.4), late exponential (OD_{650} of 0.8), or stationary phase (OD_{650} of 1.2), labeled with rabbit antibody to Ata and secondary goat antibody to rabbit IgG conjugated to Alexa 488 fluorescent dye, and analyzed by flow cytometry. Results represent the mean fluorescent intensity (MFI) of 500,000 cells, and bars indicate the averages from three independent experiments ± standard errors of the means (SEM).

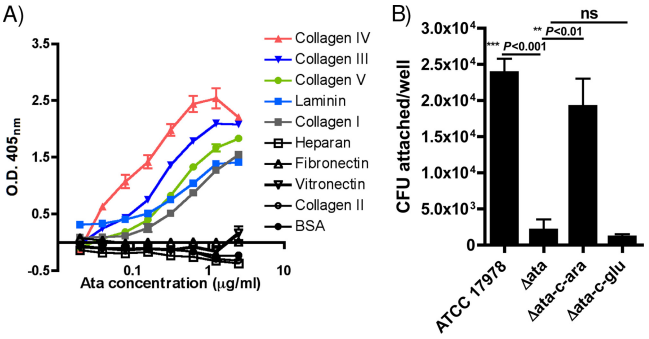

FIG 4 Adhesive properties of Ata. (A) Dose-dependent binding of Ata to selected ECM/BM components. ECM/BM proteins, including collagen types I, II, III, IV, and V, heparan, fibronectin, vitronectin, and laminin, and BSA (as a control) were used at 5 μg/well, and binding of Ata was quantified by ELISA. Data points represent the means from four independent experiments ± SEM. (B) Binding of *A. baumannii* ATCC 17978, Δ*ata*, and Δ*ata*-c induced with 2% arabinose or 0.2% glucose to immobilized collagen type IV. The bars indicate the means from three independent experiments ± SEM. *P* values were determined by one-way ANOVA with Tukey's *post hoc* analysis. ns, not significant.

multiple ECM/BMs proteins but also mediates the adhesion of *A. baumannii* cells to immobilized collagen type IV.

Ata promotes the survival of *A. baumannii in vivo*. We investigated the contribution of Ata to the virulence of *A. baumannii in vivo* by comparing the survival of wild-type *A. baumannii* ATCC 17978, Δ*ata*, Δ*ata*-pLVB-Ata (*ata* complemented in *trans* and expressed from its own promoter), and Δ*ata*-pBAD18kan-Ori (complemented with the empty plasmid) strains in a lethal model of systemic infection based on that recently described by Breslow et al. (4).

In this study, groups of eight immunocompetent mice were infected i.p. with approximately 10^7 CFU of *A. baumannii* strains, and survival was monitored for a period of 5 days. As shown in Fig. 5, infection of mice with the wild-type *A. baumannii* ATCC 17978 strain expressing Ata resulted in high levels of mortality (87.5%) compared to mice infected with the *ata*-negative strains, Δ*ata* or Δ*ata*-pBAD18kan-Ori, complemented with the empty vector, which all survived until day 5 postinfection (0% mortality; for wild-type ATCC 17978 versus Δ*ata* and ATCC 17978 versus Δ*ata*-pBAD18kan-Ori, $P = 0.0005$ by log-rank test). Surprisingly, mice infected with *A. baumannii* Δ*ata*-pLVB-Ata showed little lethality (12.5%) in this animal model.

To investigate if the reduced lethality of the *trans*-complemented strain *A. baumannii* Δ*ata*-pLVB-Ata was due to problems of stability of the complementation plasmid pLVB-Ata *in vivo*, we conducted a pilot study to assess the potential loss of pLVB-Ata from *A. baumannii* pLVB-Ata in our mouse model of lethal infection. C57BL/6 mice were infected i.p. with *A. baumannii* pLVB-Ata (2.5×10^7 CFU). Two to 3 days later animals were sacrificed, the peritoneum washed with 0.5 ml of PBS, the peritoneal lavage was plated in tryptic soy agar (TSA), and TSA plates were supplemented with kanamycin 50 μg/ml (TSA-kan). Our results revealed no significant differences in bacterial counts after growth in the presence or absence of kanamycin (480 CFU/ml TSA-kan/440

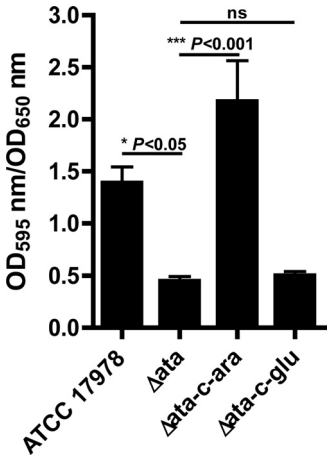

FIG 3 Quantitative biofilm formation by *A. baumannii* ATCC 17978, Δ*ata*, and Δ*ata*-c on polystyrene surfaces. *A. baumannii* 17978 and Δ*ata* were grown in LB and ATCC 17978 Δ*ata*-c in LB plus 2% arabinose or 0.2% glucose under static conditions for 24 h at 37°C. Total biofilm formation (OD_{595}) was normalized by bacterial growth (OD_{650}). The bars indicate the means of 15 tubes from five independent experiments ± SEM. *P* values were determined by one-way ANOVA with Tukey's *post hoc* analysis. ns, not significant.

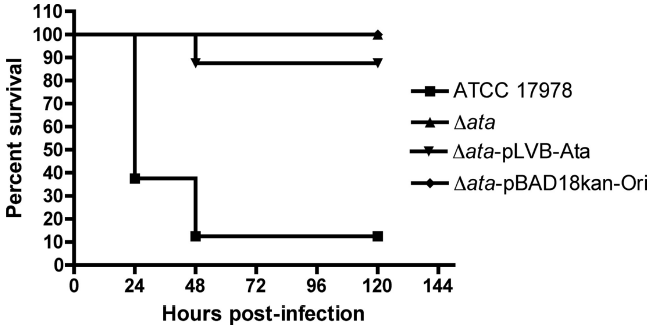

FIG 5 Survival curves of mice ($n = 8$; C57BL/6) following intraperitoneal infection with *A. baumannii* ATCC 17978 (1.6×10^7 CFU/mouse), Δ*ata* (1.6×10^7 CFU/mouse), Δ*ata*-pLVB-Ata (*ata* gene with its native promoter cloned into pBAD18Kan-Ori; 1.4×10^7 CFU/mouse), and Δ*ata*-pBAD18Kan-Ori (empty vector pBAD18Kan-Ori; 1.2×10^7 CFU/mouse). $P = 0.0005$ by log-rank test in a Kaplan-Meier analysis of wild-type ATCC 17978 versus Δ*ata* and ATCC 17978 versus Δ*ata*-pBAD18kan-Ori.

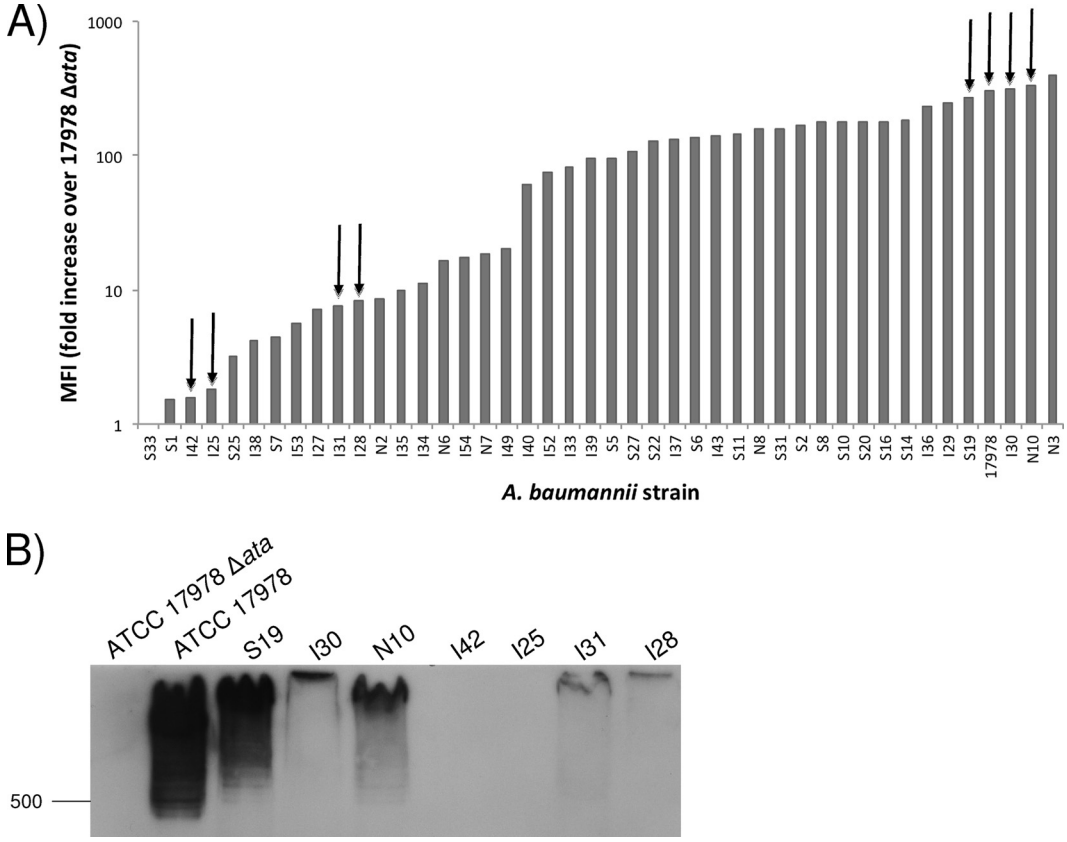

FIG 6 Analysis of Ata expression among *A. baumannii* clinical isolates. (A) Flow-cytometric analysis of Ata production among *A. baumannii* clinical isolates positive for the *ata* gene by PCR. *A. baumannii* strains were grown in LB and probed with rabbit anti-Ata antibodies and a secondary goat anti-rabbit Alexa 488 fluorescent antibody. Approximately 500,000 cells were then analyzed by flow cytometry, and antibody binding was expressed as mean fluorescent intensity (MFI). Bars represent the fold ratio (in MFI) of each *A. baumannii* clinical isolate to the MFI of the ATCC 17978 Δ*ata* strain. (B) Western blot (WB) analysis of Ata levels in 4 strains producing high levels of Ata (ATCC 17978, S19, I30, and N10) and in 4 strains producing low levels of Ata (I42, I25, I31, and I28) as determined by FACS and the Ata-negative strain ATCC 17978 Δ*ata*, which was used as a control. Migration distances of molecular mass markers (in kDa) are indicated on the left. (Strains used for WB analysis are highlighted with arrows in panel A). Outer membrane proteins were extracted, resolved by SDS-PAGE, and transferred to a PVDF membrane, and Ata was detected by WB with anti-Ata rabbit antibodies and a secondary goat anti-rabbit IgG.

CFU/ml TSA by 48 h postinfection and 30 CFU/ml TSA-kan/10 CFU/ml TSA by 72 h postinfection), indicating no plasmid loss *in vivo*.

To determine if a marginal complementation of Ata production in the *A. baumannii* Δ*ata*-pLVB-Ata strain could explain the partial *in vivo* complementation of the virulence properties, FACS analysis of Ata production among *A. baumannii* ATCC 17978, Δ*ata*, Δ*ata*-pLVB-Ata, and Δ*ata*-pBAD18kan-Ori strains was carried out. As shown in Fig. S2 in the supplemental material, the levels of Ata produced by strain *A. baumannii* Δ*ata*-pLVB-Ata were 4.4-fold lower (MFI of 16.7) than those measured in the wild-type *A. baumannii* ATCC 17978 strain (MFI of 73.8). Conversely, the *A. baumannii* Δ*ata* and Δ*ata*-pBAD18kan-Ori (empty vector) strains that do not express *ata* had very low MFI values, 3.3 and 7.3, respectively. Thus, it appears that *trans*-complementation of *ata* from its own promoter does not fully restore protein synthesis.

Ata production among clinical isolates. We determined the prevalence of the *ata* gene among *A. baumannii* strains from various geographic locations as well as clinical disease sources (lung, blood, and skin isolates). Our *A. baumannii* strain collection encompasses a total of 75 isolates obtained from American soldiers wounded in the Iraqi war (supplied by Murray Clinton), the Singapore General Hospital, (provided by Tse Hsien Koh), and serum-resistant isolates from various U.S. institutions, including the Centers for Disease Control and Prevention (CDC), the ATCC, and the University of Nebraska Medical Center (supplied to us by Paul M. Dunman). Our results showed that 44/75 (58.6%) of *A. baumannii* strains tested by PCR yielded an amplification product with an approximate size of 5.6 kb.

In addition to PCR analysis, all 44 *A. baumannii* clinical isolates positive for the *ata* gene by PCR were also tested for surface Ata production by FACS. Included in each assay as a specificity control was the ATCC 17978 Δ*ata* strain, and results were expressed as the ratio of the MFI of each strain to that of the *ata*-negative strain.

Results presented in Fig. 6A show that 43/44 *A. baumannii* strains that were positive for the *ata* gene by PCR also produced detectable surface Ata protein. The levels of Ata were high overall but varied among the *A. baumannii* clinical strains.

Although it was not surprising to find variability in the levels of Ata production among our *A. baumannii* clinical strains obtained from various geographical locations and types of infections, we decided to further investigate these findings by evaluating Ata production in outer membrane extracts of cells using Western blot

analysis. Comparing levels of Ata production by FACS and Western blotting would help to rule out some explanations for the variability observed in the levels of surface Ata, including the nonspecific binding of anti-Ata antibodies to *A. baumannii* surface components other than Ata or differences in the levels of surface exposure of the Ata protein.

We evaluated eight clinical strains of *A. baumannii* that were selected based on their FACS profiles, including four strains producing high levels of Ata (ATCC 17978, S19, I30 and N10) and four strains producing low levels of Ata (I42, I25, I31, and I28), and we included *A. baumannii* ATCC 17978 Δ*ata* as a negative control. After OMPs were extracted and Western blots were probed with anti-Ata rabbit antibodies, we found that all four strains producing high levels of Ata also had a very-high-molecular-weight reactive band, which was consistent in size with a trimer of the Ata protein (Fig. 6B). On the other hand, the four strains producing low levels of Ata as determined by FACS had low to nondetectable levels of Ata by Western blotting, and no Ata was detected in the *ata*-negative strain Δ*ata*. In addition, these immunoblot studies suggested the presence of various Ata alleles among the *A. baumannii* strains, resulting in proteins with slightly different molecular weights.

DISCUSSION

In this study, we report the identification of Ata as a TA of *A. baumannii*. Ata is surface exposed on the *A. baumannii* outer membrane, plays a role in the virulence of *A. baumannii* in mice, mediates adherence to ECM/BM proteins, and contributes to biofilm formation. Ata has all the typical features of TAs, including a long signal peptide followed by a surface-exposed passenger domain and C-terminal translocator domain encoding 4 β-strands. With a size of 1,873 amino acids per monomer, the *A. baumannii* Ata is significantly larger than other well-described TAs, such as YadA (455 aa), UspA1 (863 aa), Nhha (590 aa), and NadA (364 aa). The passenger domain of Ata encodes an RGD domain and four SVAIG, collagen-binding domains. This SVAIG motif or its derivatives are widespread among other TAs, including, for example, YadA of *Y. enterocolitica*, EmaA of *Aggregatibacter actinomycetemcomitans*, BpaA of *Burkholderia pseudomallei*, variably expressed outer membrane proteins (Vomps) of *Bartonella quintana*, and BadA of *Bartonella henselae* (43, 71, 78), among others. While the presence of SVAIG motifs is consistent with the ability of recombinant Ata to bind various types of collagens, including types I, III, IV, and V, the direct involvement of these Ata motifs in binding to collagen has not been confirmed. The RGD motif, on the other hand, is found in many adhesive proteins, including various autotransporters (22, 23, 31), and is associated with attachment to mammalian cells via binding to integrin molecules on the plasma membrane (32). The significance of this motif in adhesion and pathogenesis of *A. baumannii* has yet to be determined.

Computer predictions indicate that the β-barrel translocator of Ata forms a trimeric 12-stranded β-barrel embedded into the outer membrane with three hairpin loops, one from each Ata monomer, passing through the pore and pointing toward the extracellular space, while the α-helix fragments protrude outside. These α-helices form a neck between the membrane-inserted anchor and the surface-exposed passenger domains. Similar models have been proposed for the YadA and NhhA membrane anchor regions (63, 77).

A. baumannii frequently causes biofilm infections associated with medical devices, such as vascular catheters, cerebrospinal fluid shunts, or Foley catheters (58, 59). A number of *A. baumannii* components have been identified to be important for biofilm formation on abiotic surfaces, including the pili synthesized by the *csuA/BABCDE* chaperone-usher secretion system (73), a biofilm-associated protein (Bap) (45), and the widely distributed surface polysaccharide, poly-*N*-acetylglucosamine (PNAG) (8). We have now identified Ata as another surface component that contributes to biofilm formation in *A. baumannii*, since the deletion of this protein from the wild-type ATCC 17978 strain significantly decreases biofilm formation *in vitro*. Moreover, complementation of Ata in the Δ*ata*-c strain restored biofilm formation only when cells were grown in arabinose-inducible conditions but not in the presence of the repressible effects of glucose.

Microbial pathogens use adhesins to bind to ECM/BM macromolecules and subsequently may use them as a stronghold for propagating and spreading to other parts of the body (28). We have shown that purified recombinant Ata binds to the ECM proteins, including collagen types I, III, IV, and V and the basement protein laminin. Furthermore, this study also demonstrated that in addition to binding ECM/BM proteins, Ata mediated the adhesion of *A. baumannii* cells to immobilized collagen type IV. Collagens are the most common ECM proteins in the body, with collagen type I being the most abundant type in the human lung, and it is also prominent in the peripheral lung tissue and pulmonary vascular tissue (13). Thus, it is thought that ECM/BM components serve as docking sites for microbial pathogen invasion. We speculate that in the case of *A. baumannii* infections, ECM/BM proteins become exposed in instances where there is tissue damage, and, following adherence to ECM/BM proteins, *A. baumannii* can grow as a biofilm at these sites, making the treatment of these infections very difficult.

When we investigated the prevalence of Ata among clinical isolates of *A. baumannii*, we found that 44 of the 75 strains tested by PCR were positive for the *ata* gene (58.6%), 43 of which synthesized surface-exposed Ata by flow cytometry (56.3%).

Moreover, Western blot analysis of eight *A. baumannii* clinical isolates (four strains producing high levels of Ata and four producing low levels of Ata) demonstrated an overall good correlation between levels of Ata measured by FACS and Western blot analysis and suggested the presence of various alleles of the Ata trimers that migrated at slightly different molecular weights. Allelic variation is not uncommon in the AT family. Some examples of ATs that display allelic diversity include Ag43 in *E. coli* (74), UspA in *M. catarrhalis* (5), NadA in *N. meningitidis* (14), and VacA (17), BabA, and BabB (57) in *Helicobacter pylori*, among others. Studies are now under way to investigate if the lack of amplification of *ata* in a subset of *A. baumannii* strains using a primer set designed based on sequenced strain ATCC 17978 is due to sequence divergence, gene localization in the chromosome, or the true absence of the *ata* gene.

This work also presents clear evidence of the surface exposure of Ata in *A. baumannii*, as the CLSM and FACS studies were carried out using intact, unpermeabilized bacterial cells. Moreover, the role of Ata in biofilm formation, adhesion to collagen type IV, and mouse virulence provide additional indications of its surface exposure.

Due to the overall low virulence of most *A. baumannii* strains in rodent models of infection, investigators have used various

methods to enhance virulence, including mixing bacterial inocula with porcine mucin (49, 60) or the use of neutropenic mouse models of *A. baumannii* infections (36, 67, 75). However, neutropenia is a rare clinical risk factor for patients with *A. baumannii* infections (1a, 6, 7, 20, 26, 34, 40, 50), and therefore an alternative model of *A. baumannii* infection in immunocompetent animals is desirable to more accurately mimic the types of infections caused by this organism. For these reasons, we chose an immunocompetent mouse model of infection based on that recently developed by Breslow et al. (4) to evaluate the role of Ata in *A. baumannii* virulence. In this animal model, infections are induced via i.p. injection and *A. baumannii* virulence assessed by mortality during a 5-day period.

Using this lethal model of systemic infection, we could demonstrate the role of Ata in *A. baumannii* virulence. As shown, the deletion of *ata* from wild-type *A. baumannii* ATCC 17978 significantly decreased the virulence of this strain in the murine model of lethal infection. However, *trans*-complementation of Ata in the plasmid pLVB-Ata only marginally restored the virulence of the wild-type strain.

Considerable effort has been focused on the construction of a complementation plasmid suitable for *in vivo* studies aimed at investigating the role of Ata in *A. baumannii* virulence. After testing various vectors for complementation, we constructed the plasmid pLVB-Ata, carrying the *ata* gene, with its native promoter in the shuttle vector pBAD18kan-Ori. The pLVB-Ata plasmid was highly stable *in vivo* in the strain *A. baumannii* Δ*ata*-pLVB-Ata, even in the absence of antibiotic selection in our mouse model of lethal infection. Despite these encouraging results, FACS levels of Ata production *in vitro* in *A. baumannii* Δ*ata*-pLVB-Ata were 4.4-fold lower than those seen in the wild-type *A. baumannii* ATCC 17978 strain. Although the nature of this reduced complementation remains unclear, we speculate that an undetermined *cis*-regulatory element is required for the regulation of Ata, which would explain the limited *trans*-complementation of virulence seen in the *A. baumannii* Δ*ata*-pLVB-Ata strain, where *ata* is expressed from its native promoter in the stable plasmid pBAD18kan-Ori.

Therefore, our findings are consistent overall with the conclusion that Ata plays a role in *A. baumannii* virulence as determined in a murine lethal model of infection, promoting biofilm formation and ECM/BM protein binding and mediating the adhesion of *A. baumannii* cells to immobilized collagen type IV. These findings may help promote the development of novel therapeutic strategies to limit *A. baumannii*-associated morbidity and mortality.

ACKNOWLEDGMENTS

We acknowledge the contributions to this work of Lai Ding (Optical Imaging Core Facility, Harvard Medical School) for his help with the CLSM studies and Valeria Risso for her assistance in generating a computer model of the 3D structure of the Ata translocator domain using the Chimera computer modeling tool.

This work was supported by NIH grant AI 046706.

REFERENCES

1. **American Association for Pediatrics.** 2006. Pertussis (whooping cough). Red Book Online **2006**:498–520.
1a. **Beavers SF, et al.** 2009. Comparison of risk factors for recovery of *Acinetobacter baumannii* during outbreaks at two Kentucky hospitals, 2006. Public Health Rep. **124**:868–874.
2. **Bendtsen JD, Nielsen H, von Heijne G, Brunak S.** 2004. Improved prediction of signal peptides: SignalP 3.0. J. Mol. Biol. **340**:783–795.
3. **Bradford MM.** 1976. A rapid and sensitive method for the quantitation of microgram quantities of protein utilizing the principle of protein-dye binding. Anal. Biochem. **72**:248–254.
4. **Breslow JM, et al.** 2011. Innate immune responses to systemic *Acinetobacter baumannii* infection in mice: neutrophils, but not interleukin-17, mediate host resistance. Infect. Immun. **79**:3317–3327.
5. **Brooks MJ, et al.** 2008. Modular arrangement of allelic variants explains the divergence in *Moraxella catarrhalis* UspA protein function. Infect. Immun. **76**:5330–5340.
6. **Caricato A, et al.** 2009. Risk factors and outcome of *Acinetobacter baumanii* infection in severe trauma patients. Intensive Care Med. **35**:1964–1969.
7. **Chiang D-H, et al.** 2008. Risk factors for mortality in patients with *Acinetobacter baumannii* bloodstream infection with genotypic species identification. J. Microbiol. Immunol. Infect. **41**:397–402.
8. **Choi AHK, Slamti L, Avci FY, Pier GB, Maira-Litran T.** 2009. The *pgaABCD* locus of *Acinetobacter baumannii* encodes the production of poly-β-1-6-N-acetylglucosamine, which is critical for biofilm formation. J. Bacteriol. **191**:5953–5963.
9. **Choi CH, et al.** 2008. *Acinetobacter baumannii* outer membrane protein A targets the nucleus and induces cytotoxicity. Cell Microbiol. **10**:309–319.
10. **Choi CH, et al.** 2005. Outer membrane protein 38 of *Acinetobacter baumannii* localizes to the mitochondria and induces apoptosis of epithelial cells. Cell Microbiol. **7**:1127–1138.
11. **Choi CH, Lee JS, Lee YC, Park TI, Lee JC.** 2008. *Acinetobacter baumannii* invades epithelial cells and outer membrane protein A mediates interactions with epithelial cells. BMC Microbiol. **8**:216. doi:10.1186/1471-2180-8-216.
12. **Cisneros JM, et al.** 1996. Bacteremia due to *Acinetobacter baumannii*: epidemiology, clinical findings, and prognostic features. Clin. Infect. Dis. **22**:1026–1032.
13. **Clark JG, Kuhn C, McDonald JA, Mecham RP.** 1983. Lung connective tissue. Int. Rev. Connect. Tissue Res. **10**:249–331.
14. **Comanducci M, et al.** 2002. NadA, a novel vaccine candidate of *Neisseria meningitidis*. J. Exp. Med. **195**:1445–1454.
15. **Costerton JW, Stewart PS, Greenberg EP.** 1999. Bacterial biofilms: a common cause of persistent infections. Science **284**:1318–1322.
16. **Cotter SE, Surana NK, St Geme JW.** 2005. Trimeric autotransporters: a distinct subfamily of autotransporter proteins. Trends Microbiol. **13**:199–205.
17. **Cover TL, Tummuru MK, Cao P, Thompson SA, Blaser MJ.** 1994. Divergence of genetic sequences for the vacuolating cytotoxin among *Helicobacter pylori* strains. J. Biol. Chem. **269**:10566–10573.
18. **Davis KA, Moran KA, McAllister CK, Gray PJ.** 2005. Multidrug-resistant Acinetobacter extremity infections in soldiers. Emerg. Infect. Dis. **11**:1218–1224.
19. **Dijkshoorn L, Nemec A, Seifert H.** 2007. An increasing threat in hospitals: multidrug-resistant *Acinetobacter baumannii*. Nat. Rev. Microbiol. **5**:939–951.
20. **Dizbay M, Tunçcan OG, Sezer BE, Hizel K.** 2010. Nosocomial imipenem-resistant *Acinetobacter baumannii* infections: epidemiology and risk factors. Scand. J. Infect. Dis. **42**:741–746.
21. **Donlan RM, Costerton JW.** 2002. Biofilms: survival mechanisms of clinically relevant microorganisms. Clin. Microbiol. Rev. **15**:167–193.
22. **D'Souza SE, Ginsberg MH, Burke TA, Lam SC, Plow EF.** 1988. Localization of an Arg-Gly-Asp recognition site within an integrin adhesion receptor. Science **242**:91–93.
23. **Finn TM, Stevens LA.** 1995. Tracheal colonization factor: a *Bordetella pertussis* secreted virulence determinant. Mol. Microbiol. **16**:625–634.
24. **Gaddy JA, Tomaras AP, Actis LA.** 2009. The *Acinetobacter baumannii* 19606 OmpA protein plays a role in biofilm formation on abiotic surfaces and in the interaction of this pathogen with eukaryotic cells. Infect. Immun. **77**:3150–3160.
25. **Garcia-Garmendia J, et al.** 2001. Risk factors for *Acinetobacter baumannii* nosocomial bacteremia in critically ill patients: a cohort study. Clin. Infect. Dis. **33**:939–946.
26. **Gómez J, et al.** 1999. Six-year prospective study of risk and prognostic factors in patients with nosocomial sepsis caused by *Acinetobacter baumannii*. Eur. J. Clin. Microbiol. Infect. Dis. **18**:358–361.
27. **Guex N, Peitsch MC.** 1997. SWISS-MODEL and the Swiss-PdbViewer: an environment for comparative protein modeling. Electrophoresis **18**:2714–2723.
28. **Hauck CR, Agerer F, Muenzner P, Schmitter T.** 2006. Cellular adhesion molecules as targets for bacterial infection. Eur. J. Cell Biol. **85**:235–242.

29. **Hawley JS, et al.** 2007. Susceptibility of acinetobacter strains isolated from deployed U.S. military personnel. Antimicrob. Agents Chemother. **51**: 376–378.
30. **Hellwig SMM, Rodriguez ME, Berbers GAM, van de Winkel JGJ, Mooi FR.** 2003. Crucial role of antibodies to pertactin in *Bordetella pertussis* immunity. J. Infect. Dis. **188**:738–742.
31. **Henderson IR, Owen P.** 1999. The major phase-variable outer membrane protein of *Escherichia coli* structurally resembles the immunoglobulin A1 protease class of exported protein and is regulated by a novel mechanism involving Dam and oxyR. J. Bacteriol. **181**:2132–2141.
32. **Humphries J, Byron A.** 2006. Integrin ligands at a glance. J. Cell Sci. **119**:3901–3903.
33. **Jacobs AC, et al.** 2010. Inactivation of phospholipase D diminishes *Acinetobacter baumannii* pathogenesis. Infect. Immun. **78**:1952–1962.
34. **Jang TN, Lee SH, Huang CH, Lee CL, Chen WY.** 2009. Risk factors and impact of nosocomial *Acinetobacter baumannii* bloodstream infections in the adult intensive care unit: a case-control study. J. Hosp. Infect. **73**:143–150.
35. **Jin JS, et al.** 2011. *Acinetobacter baumannii* secretes cytotoxic outer membrane protein A via outer membrane vesicles. PLoS One **6**:e17027. doi: 10.1371/journal.pone.0017027.
36. **Joly-Guillou ML, Wolff M, Pocidalo JJ, Walker F, Carbon C.** 1997. Use of a new mouse model of *Acinetobacter baumannii* pneumonia to evaluate the postantibiotic effect of imipenem. Antimicrob. Agents Chemother. **41**:345–351.
37. Reference deleted.
38. **Jones DT.** 2007. Improving the accuracy of transmembrane protein topology prediction using evolutionary information. Bioinformatics **23**: 538–544.
39. **Kapoor R.** 2008. Acinetobacter infection. N. Engl. J. Med. **358**:2845–2847.
40. **Lautenbach E, et al.** 2009. Epidemiology and impact of imipenem resistance in *Acinetobacter baumannii*. Infect. Control Hosp. Epidemiol. **30**: 1186–1192.
41. **Lee H-W, et al.** 2008. Capacity of multidrug-resistant clinical isolates of A*cinetobacter baumannii* to form biofilm and adhere to epithelial cell surfaces. Clin. Microbiol. Infect. **14**:49–54.
42. **Lee JC, et al.** 2006. Adherence of *Acinetobacter baumannii* strains to human bronchial epithelial cells. Res. Microbiol. **157**:360–366.
43. **Linke D, Riess T, Autenrieth IB, Lupas A, Kempf VAJ.** 2006. Trimeric autotransporter adhesins: variable structure, common function. Trends Microbiol. **14**:264–270.
44. **Livak K.** 2001. Analysis of relative gene expression data using real-time quantitative PCR and the $2-\Delta\Delta$ CT method. Methods **25**:402–408.
45. **Loehfelm TW, Luke NR, Campagnari AA.** 2008. Identification and characterization of an *Acinetobacter baumannii* biofilm-associated protein. J. Bacteriol. **190**:1036–1044.
46. Reference deleted.
47. **Maira-Litran T, Kropec A, Goldmann DA, Pier GB.** 2005. Comparative opsonic and protective activities of *Staphylococcus aureus* conjugate vaccines containing native or deacetylated staphylococcal poly-N-acetyl-beta-(1-6)-glucosamine. Infect. Immun. **73**:6752–6762.
48. **Maragakis LL, Perl TM.** 2008. *Acinetobacter baumannii*: epidemiology, antimicrobial resistance, and treatment options. Clin. Infect. Dis. **46**: 1254–1263.
49. **McConnell MJ, et al.** 2011. Vaccination with outer membrane complexes elicits rapid protective immunity to multidrug-resistant *Acinetobacter baumannii*. Infect. Immun. **79**:518–526.
50. **Metan G, Sariguzel F, Sumerkan B.** 2009. Factors influencing survival in patients with multi-drug-resistant Acinetobacter bacteraemia. Eur. J. Intern. Med. **20**:540–544.
51. **Nielsen M, Lundegaard C, Lund O, Petersen TN.** 2010. CPHmodels-3.0–remote homology modeling using structure-guided sequence profiles. Nucleic Acids Res. **38**:W576–W581.
52. **Nishimura K, Tajima N, Yoon Y-H, Park S-Y, Tame JRH.** 2010. Autotransporter passenger proteins: virulence factors with common structural themes. J. Mol. Med. **88**:451–458.
53. **Oncül O, et al.** 2002. Hospital-acquired infections following the 1999 Marmara earthquake. J. Hosp. Infect. **51**:47–51.
54. **Peleg AY, Seifert H, Paterson DL.** 2008. *Acinetobacter baumannii*: emergence of a successful pathogen. Clin. Microb. Rev. **21**:538–582.
55. **Perez F, et al.** 2007. Global challenge of multidrug-resistant *Acinetobacter baumannii*. Antimicrob. Agents Chemother. **51**:3471–3484.
56. **Pettersen EF, et al.** 2004. UCSF Chimera–a visualization system for exploratory research and analysis. J. Comput. Chem. **25**:1605–1612.
57. **Pride DT, Meinersmann RJ, Blaser MJ.** 2001. Allelic variation within *Helicobacter pylori* babA and babB. Infect. Immun. **69**:1160–1171.
58. **Richet H, Fournier PE.** 2006. Nosocomial infections caused by *Acinetobacter baumannii:* a major threat worldwide. Infect. Control Hosp. Epidemiol. **27**:645–646.
59. **Rodríguez-Baño J, et al.** 2004. Clinical features and epidemiology of *Acinetobacter baumannii* colonization and infection in Spanish hospitals. Infect. Control Hosp. Epidemiol. **25**:819–824.
60. **Rodríguez-Hernández MJ, et al.** 2000. Imipenem, doxycycline and amikacin in monotherapy and in combination in *Acinetobacter baumannii* experimental pneumonia. J. Antimicrob. Chemother. **45**:493–501.
61. **Roggenkamp A, et al.** 2003. Molecular analysis of transport and oligomerization of the *Yersinia enterocolitica* adhesin YadA. J. Bacteriol. **185**: 3735–3744.
62. **Russo TA, et al.** 2010. The K1 capsular polysaccharide of *Acinetobacter baumannii* strain 307-0294 is a major virulence factor. Infect. Immun. **78**:3993–4000.
63. **Scarselli M, et al.** 2006. *Neisseria meningitidis* NhhA is a multifunctional trimeric autotransporter adhesin. Mol. Microbiol. **61**:631–644.
64. **Seifert H, Strate A, Pulverer G.** 1995. Nosocomial bacteremia due to *Acinetobacter baumannii*. Clinical features, epidemiology, and predictors of mortality. Medicine **74**:340–349.
65. **Serruto D, et al.** 2010. *Neisseria meningitidis* GNA2132, a heparin-binding protein that induces protective immunity in humans. Proc. Natl. Acad. Sci. U. S. A. **107**:3770–3775.
66. **Smith MG, et al.** 2007. New insights into *Acinetobacter baumannii* pathogenesis revealed by high-density pyrosequencing and transposon mutagenesis. Genes Dev. **21**:601–614.
67. **Song JY, Cheong HJ, Lee J, Sung AK, Kim WJ.** 2009. Efficacy of monotherapy and combined antibiotic therapy for carbapenem-resistant *Acinetobacter baumannii* pneumonia in an immunosuppressed mouse model. Int. J. Antimicrob. Agents **33**:33–39.
68. **Steyert SR, Pineiro SA.** 2007. Development of a novel genetic system to create markerless deletion mutants of *Bdellovibrio bacteriovorus*. Appl. Environ. Microbiol. **73**:4717–4724.
69. **St Geme JW, Kumar VV, Cutter D, Barenkamp SJ.** 1998. Prevalence and distribution of the *hmw* and *hia* genes and the HMW and Hia adhesins among genetically diverse strains of nontypeable *Haemophilus influenzae*. Infect. Immun. **66**:364–368.
70. **Surana NK, Cutter D, Barenkamp SJ, St Geme JW.** 2004. The *Haemophilus influenzae* Hia autotransporter contains an unusually short trimeric translocator domain. J. Biol. Chem. **279**:14679–14685.
71. **Tahir YE, Kuusela P, Skurnik M.** 2000. Functional mapping of the Yersinia enterocolitica adhesin YadA. Identification of eight NSVAIG-S motifs in the amino-terminal half of the protein involved in collagen binding. Mol. Microbiol. **37**:192–206.
72. **Tien HC, et al.** 2007. Multi-drug resistant *Acinetobacter infections* in critically injured Canadian forces soldiers. BMC Infect. Dis. **7**:95. doi: 10.1186/1471-2334-7-95.
73. **Tomaras AP, Dorsey CW, Edelmann RE, Actis LA.** 2003. Attachment to and biofilm formation on abiotic surfaces by *Acinetobacter baumannii*: involvement of a novel chaperone-usher pili assembly system. Microbiology **149**:3473–3484.
74. **van der Woude MW, Henderson IR.** 2008. Regulation and function of Ag43 (Flu). Annu. Rev. Microbiol. **62**:153–169.
75. **van Faassen H, et al.** 2007. Neutrophils play an important role in host resistance to respiratory infection with *Acinetobacter baumannii* in mice. Infect. Immun. **75**:5597–5608.
76. **Wang Y, et al.** 2010. Causes of Infection after earthquake, China, 2008. Emerging Infect. Dis. **16**:974–975.
77. **Wollmann P, Zeth K, Lupas AN, Linke D.** 2006. Purification of the YadA membrane anchor for secondary structure analysis and crystallization. Int. J. Biol. Macromol. **39**:3–9.
78. **Zhang P, et al.** 2004. A family of variably expressed outer-membrane proteins (Vomp) mediates adhesion and autoaggregation in *Bartonella quintana*. Proc. Natl. Acad. Sci. U. S. A. **101**:13630–13635.
79. **Zimbler DL, et al.** 2009. Iron acquisition functions expressed by the human pathogen *Acinetobacter baumannii*. Biometals **22**:23–32.